

Lawrence Berkeley National Laboratory

LBL Publications

Title

Wellbore integrity assessment with casing-based advanced sensing

Permalink

<https://escholarship.org/uc/item/849853k9>

Authors

Wilt, Michael

Um, Evan

Weiss, Chester

et al.

Publication Date

2021-10-26

Peer reviewed

Wellbore Integrity Assessment with Casing-Based Advanced Sensing

Michael Wilt^{1*}, Evan Um¹, Chester Weiss², Don Vasco¹, Petr Petrov¹, Greg Newman¹, Yuxin Wu¹

¹Lawrence Berkeley National Lab, Berkeley CA 94720

²Sandia National Laboratories, Albuquerque, NM 87123

mwilt@lbl.gov

Keywords: well integrity, geophysics, infrastructure, electromagnetics, electrostatics, seismics, numerical modeling

ABSTRACT

Wellbore integrity is of paramount importance to subsurface resource extraction, energy storage¹ and waste disposal. After installation, well casing and cement are subject to mechanical stress due to near-well pressure changes and fluid induced corrosion. This is exacerbated for geothermal wells where produced fluid is at high temperature and corrosive. The current state-of-the-art technologies for wellbore integrity assessments are an array of cased hole logging tools. Wireline deployed acoustic, electromagnetic and mechanical tools are all available to inspect steel casing corrosion and casing-cement bond and these tools can provide high-resolution assessment of borehole conditions. They are intrusive, however, in terms of borehole preparation and interruption to the normal operation of the wells, and not suitable for high temperature or highly deviated well deployments. In addition, these measurements are performed infrequently due to high cost, and are therefore incapable of providing frequent data to better predict borehole degradation trajectory, which can help provide early warning of potential borehole failures.

For this project we are developing a suite of novel, non-invasive, casing based tools for wellbore integrity assessment, combining fast/low cost screening with higher-precision investigation. Our approach is based on monitoring the response of the casing when energized at the wellhead, thereby interrogating the casing without well intervention. Lab, field and numerical approaches are used in our study. During the early stage of the research, we focus on numerical simulations, which have shown the sensitivity of the low frequency electromagnetic (EM) signals to changes in borehole depths and have successfully tested the concept at a field site with different length well casings. Initial seismic modeling efforts have also demonstrated our capability to simulate seismic tube wave and seismic field alterations due to borehole breakage and associated fluid leakage. Further numerical, laboratory and field experiments are underway for additional technology sensitivity analysis, particularly the transient EM/Seismic reflectometry methods, data acquisition optimization, and numerical simulation improvements.

1. INTRODUCTION

Wellbore integrity is of paramount importance to subsurface resource extraction, energy storage and waste disposal. After installation, the casing and cement are subject to mechanical stress due to near-well pressure changes and fluid induced corrosion. This is exacerbated for geothermal and carbon-capture and storage (CCS) wells where produced water is at high temperature or contains dissolved CO₂ and H₂S, which can accelerate corrosion rates. Impaired wellbores could result in reduced productivity, early abandonment and leakage (e.g. CO₂, methane or other hydrocarbons) that can cause significant damages to both humans and the environment, as witnessed during the recent Aliso Canyon gas leakage events (Conley et. al., 2016). Recent studies have shown more than 1 million wells in the US have significant completion degradation and many of these are leaking (Ingraffea et al., 2014).

Effective wellbore integrity monitoring is critical for assessing the borehole state of health, identifying damaged zones for remedial actions and guiding decision-making. In addition to the deep and often pressurized boreholes that are not easily accessible, technologies for wellbore integrity monitoring are further challenged with complex subsurface geology, geochemistry and stress conditions that result in extreme variability of damage rate, pattern, magnitude and depth among different wells. The current state-of-the-art technologies for wellbore integrity assessments are an array of cased hole logging tools. Wireline deployed acoustic, electromagnetic and mechanical tools are all available to inspect steel casing corrosion and casing-cement bond and these tools can provide high-resolution assessment of borehole conditions. They are intrusive, however, in terms of borehole preparation and interruption to the normal operation of the wells and not suitable for high temperature or highly deviated well deployments. In addition, these measurements are expensive to obtain and are, thus, performed infrequently which, in most cases, are only when problems with the wells have already occurred. These limitations render the downhole wireline tools incapable of providing frequent monitoring data in order to better predict borehole degradation trajectory, which can help provide early warning of potential borehole failures.

For this project we are developing a novel, non-invasive, approach for wellbore integrity assessment. The technologies proposed combine fast/low cost screening with higher-precision investigation and are based on monitoring the response of the casing when energized at the wellhead, thereby interrogating the casing without well intervention (Figure 1). Specifically, we integrate a suite of geophysical and electrochemical methods, including direct current (DC) and low frequency electromagnetic imaging (DC-EMI), transient EM and acoustic pulse reflectometry (EMPR and APR) and electrochemical sensing based on half-cell potential (HCP) measurements. Specifically, DC-EMI and electrochemical sensing can provide fast casing health screening, and the pulse reflectometry methods can provide higher precision location of wellbore irregularity in CCS, geothermal or hydrocarbon and other type.

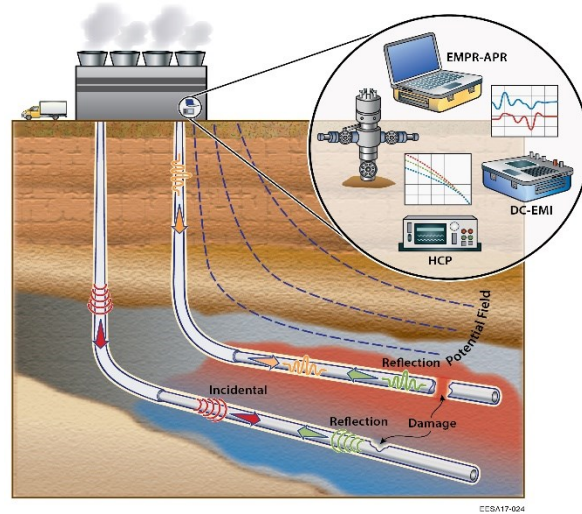


Figure 1: Concepts of the data acquisition system combining low frequency EM with transient EM/Seismic reflectometry and electrochemical measurements.

2. METHODS

2.1 Low frequency EM method:

An important aspect of this project involves using EM fields, emanating from a wellhead source, to assess the integrity of a well casing without the requirement of entering the well. The concept utilizes the principle that the majority of the current impressed will remain on the casing until the string is terminated into the full well depth, or interrupted by broken or corroded casing. Analysis of the resulting EM profile will therefore be diagnostic on the condition of the well casing. Here we discuss the development and validation of the modeling codes, the use of these codes for survey design and the application of our system to field site where EM profiles were measured from wells of different casing depth.

2.1.1 EM Numerical Modeling

Electromagnetic modeling in the presence of steel infrastructures such as cased wells and pipes is difficult because of their hollow geometry and extreme conductivity contrast. Code EM3D is a 3D finite element code capable of modeling the response of EM source in an arbitrary 3D earth, which includes metallic well casing and infrastructure. To overcome the modeling challenges associated with steel infrastructure, we use 3D modeling algorithms with tetrahedral meshes (Um et al., 2017). Tetrahedral meshes allow efficient local refinements in the computational domain such that fine meshes can be used around arbitrarily complex wells for accurate solution and coarse meshes elsewhere for efficient solutions. The EM3D code is an important tool in the validation of the EM method, establishing sensitivity to casing completion and in the design of field surveys.

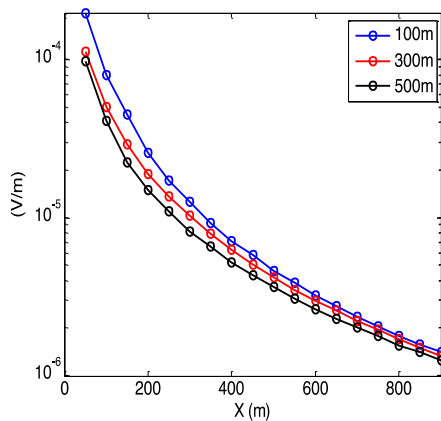


Figure 2: EM amplitude vs offset for a variety of casing depths

In Figure 2, we plot profile data from EM3D for a series of simple casing models in a cylindrical geometry with a distant (5 km) return electrode. The figure illustrates a strong dependence of the field amplitude with the depth of well casing. We note that due to the current discontinuity, a broken or highly corroded pipe has the same EM characteristics as the upper (unbroken) section of well casing. We view EM3D as a practical tool to model the field profile distribution from a steel-cased well in a conductive earth. The code allows for complex well completion and a 3D background earth, allows for a local return electrode that can model the effect of other infrastructure such as nearby wellheads and pipelines. In addition, the code allows for computation at multiple frequencies.

2.1.2 Electrostatic Modeling

In settings where the excitation frequency is low or the background conductivity is low, electrostatic modeling can be sufficiently accurate for casing integrity calculation and it is an extremely powerful tool for modeling adjacent infrastructure (see Figure 3). Modeling electrostatic response is much less computationally burdensome than broadband response with similar flexibility in model discretization. Recent advances in finite element analysis (Weiss, 2017) allow for the borehole casing to be economically represented by the infinitely thin edges — each connected to its neighbor to form an arbitrarily sinuous borehole path — rather than volumetric discretization of the casing volume itself. In doing so, the savings in computational resources are profound: rather than ~ 7 million elements per kilometer for 20cm borehole discretization (including the fluid-filled interior), the edge discretization can be done with node spacing on the order of 10 m, the equivalent length of one section of borehole casing. Hence, highly complex models are now feasible to evaluate on a modest laptop (Figure 3). This includes multiple storage tanks, surface pipelines and 122 steel cased wells. 35km of steel pipe/casing in the model is discretized at 10 m spacing. The runtime on a laptop is a few minutes; the projected runtime using volume discretization is estimated at over 2 months on the same machine (Weiss and Wilson, 2017).

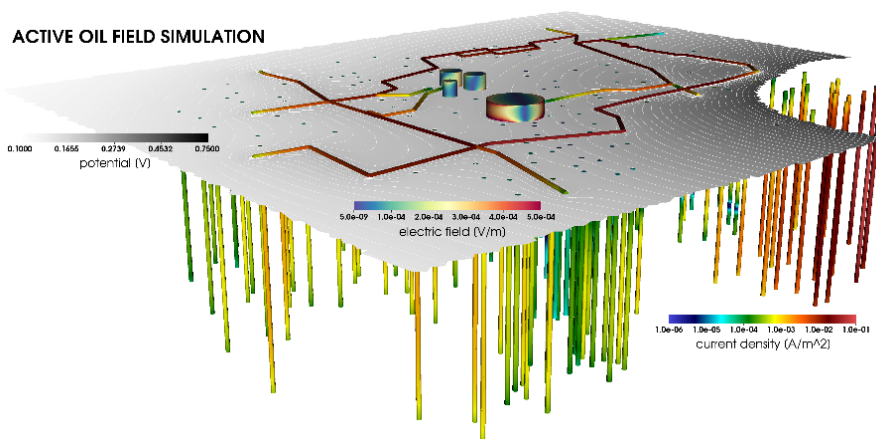


Figure 3: Example calculation using the hierarchical model representation to model the electrostatic response of an “as-built” oilfield setting,

2.1.3 EM/Seismic Reflectometry monitoring

Reflectometry has been used for decades for locating faults on electrically conductive wires and cables or pipes (Furse et al., 2009; Amir et al., 2010). It is a non-invasive method that works by sending a pulse of incidental signal (e.g. EM or acoustic) down the wire/pipe under test and records the reflected signal off impedance changes due to anomalies such as corrosion, breaks or short/open circuits. The time delay and nature (e.g. shape, polarity and magnitude) of the reflection is proportional to the distance to and the characteristics (e.g. damage severity) of the faults.

Rather than the actual distance, the recorded raw data provides the time delay between the incidental and reflected signals during reflectometry measurements. The distance to discontinuity is calculated based on the velocity of the signal propagation and the time delay. For EM pulse reflectometry, while developed for applications in electrical and civil engineering, it can be used as non-invasive tools for wellbore integrity monitoring. The steel casing acts as a long electrical conductor that can guide the propagation of incident signals applied at the wellhead. Corrosion/stress induced casing degradation can result in changes of casing impedance, which can generate reflections of the incidental signals. The reflected signals are recorded at the wellhead to provide precise position and the characteristics (e.g. magnitude of corrosion or damage) of these discontinuities. Similar to the EM method, seismic reflectometry is based on the propagation of seismic tube wave along the borehole and its reflection recorded at the wellhead. While they are often considered noise in cross well seismic survey or vertical seismic profiling, they are sensitive to the alteration of the wellbore casing, such as casing shear or damage due to stress/corrosion (Alexandrov et al., 2007), thus can be utilized to monitor casing conditions. Numerical models have simulated tube wave propagation and explored its sensitivity to casing conditions (e.g. corrosion, fractures) (Alexandrov et al., 2007; Ponomarenko, 2008). Little has been done experimentally to explicitly correlate tube wave reflection with casing conditions.

3. RESULTS

3.1 Field Application at CaMI field site:

Lawrence Berkeley National Laboratory is collaborating with the Containment and Monitoring Institute (CaMI) of the University of Calgary in mapping and monitoring an intermediate depth CO_2 injection in southern Alberta Canada. CO_2 is injected at a rate of up to one ton/day, to study monitoring technology and detection of gas-phase CO_2 in an intermediate-depth, leakage-analog experiment. The CaMI site has two dedicated monitoring wells instrumented with surface and downhole pressure, temperature, strain, seismic and electrical sensors for periodic measurement of subsurface changes associated with CO_2 injection.

Figure 4 displays the infrastructure at the CaMI site. The site features three co-linear vertical wells overlying a long linear trench containing electrodes and fiber-optic cables. The central well is a 550m steel-cased deep borehole where CO_2 will be injected from the nearby tank into a subsurface aquifer. The outer two boreholes are observation wells. OB1 is a steel-cased well completed to 350m;

OB2 has a shallow steel cased section, which crosses over to a fiberglass-cased section at a depth of 58m. Except for the injection well the boreholes are isolated from the metallic and electrical infrastructure.

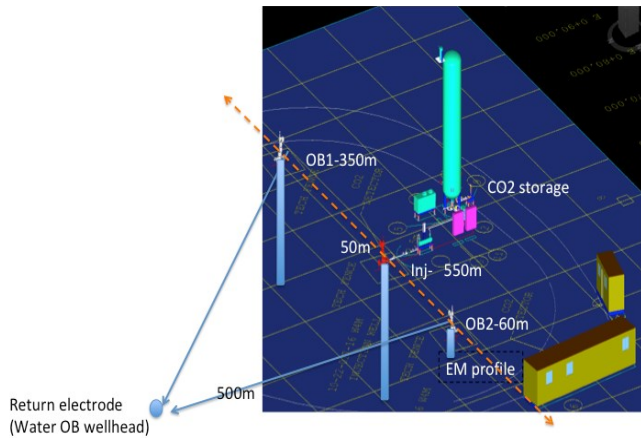


Figure 4: Map of the infrastructure at the CaMI site.

A preliminary simulation of the electrostatic potential in log scale around OB2 using a DC wellhead source is given in Figure 5. The tetrahedral mesh was constructed using CUBIT (www.sandia.gov) which consisted of ~67k nodes and ~350k tetrahedra, with the measurement profile discretized on 1 m spacing. The overall computational domain is a 10 x 10 x 5 km block and the calculation required only 15s on a laptop computer. Each colored region represents a factor 10 on in voltage. The brown region in Figure 5 surrounds the shallow OBS2 well, next to which one can clearly see the much deeper INJ and OBS1 wells. Also evident is dense node spacing on the profile line. Numerical experiments with coarser spacings (~5m) achieved similar results, albeit lacking some of the fidelity offered by 1 m spacing in the vicinity of the well heads.

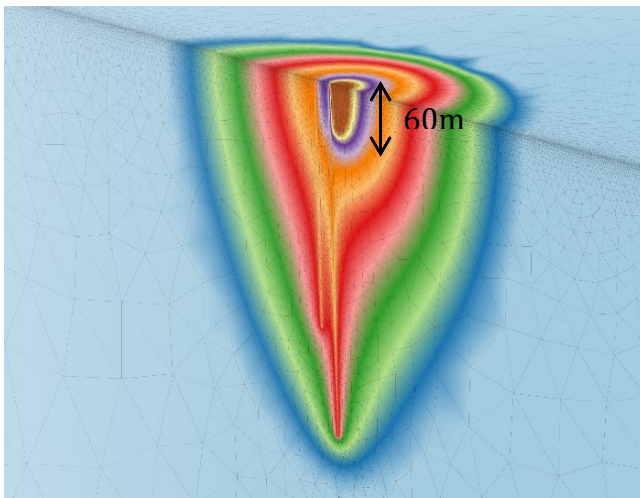


Figure 5: Cut-away view through the profile line of electric potential, color scale restricted to +’ve values, for excitation of the OBS2 well

Our field trial consisted of energizing the casing at the top of wells OB1 and OB2 in turn, using a 1-amp current and measuring the resulting voltage on the array of trench electrodes. For the source we connected a known signal to the top of the well casing with standard electrical wire and a return electrode located 500m to the northwest along a line perpendicular to the line of electrodes at well OB2. The 5Hz sine wave signal was generated using a portable power amplifier connected to a signal generator. Electrode voltages were measured using a 24 channel Geometrics “Geode” system which collected the data separately from each of the 7, 16 channel cables. Signals were averaged 100 times for each run and usually 2-4 runs were made for each cable. The entire field collection for both wells heads required about 2 hours. We were careful to ensure that the source and receiver power systems were well isolated electrically and by powering each from a separate source.

Raw data profiles for the OB1 and OB2 profiles are shown in Figure 6. Here we plot the electric field amplitude in V/m from each profile. Note that the wellhead for OB2 is located along the profiles at 500m, for OB1 the wellhead is at 550m. Each of the profiles display the characteristic decay away from the source well. In general, the data quality was excellent for both profiles, with data repeating to 1 percent or better for all but the most distant electrodes. We make the following observations about the data below.

- The maximum electric field value for profile OB2 is roughly 1 V/m, or about 5 times larger than the level for OB1. This difference is both expected and encouraging. The profile fields are a strong function of the current on the well casing and this current is larger for a shorter casing (OB2), which results in much larger profile field values.
- The profiles shape for profile OB2 is roughly symmetric but not so for OB1. This is due to the position of the return electrode, which is aligned perpendicular to the profile line at well OB2 (Figure 4).
- We note that points that deviate from the main profile curve are seen at the same locations on both profiles and these are also repeatable to about 1%. These excursions are mainly due to coupling to infrastructure such as wellheads, and pipelines. In several cases, we can fit the excursions to models (see Figures 7 and 8).

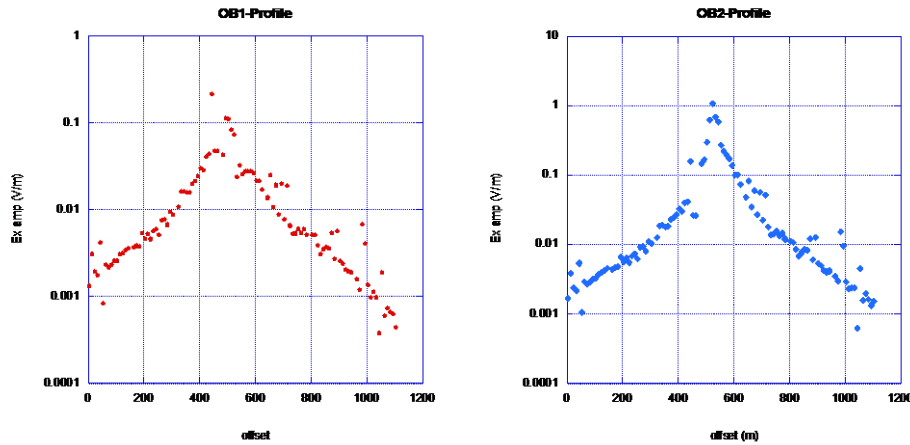


Figure 6: Electrical field amplitude surface profiles for wells OB1 and OB2

3.2.1 Fitting CaMI field data to numerical models

To validate our measurements we compare the results to a numerical model. Here we applied EM3D using completion diagram supplied by CaMI and a background resistivity consistent with the borehole logs. It was also important to use the accurate position of the return electrode. We note that for the data fit, the code also incorporated well casings for the injection well and the other observation well, either OB1 or OB2, in the calculation.

The fit of the observed data to the calculated response is impressively close considering the approximate knowledge of the background resistivity (Figure 7). We note that several of the excursions, especially at longer offsets were not fit mainly because the infrastructure that likely caused them not being well mapped.

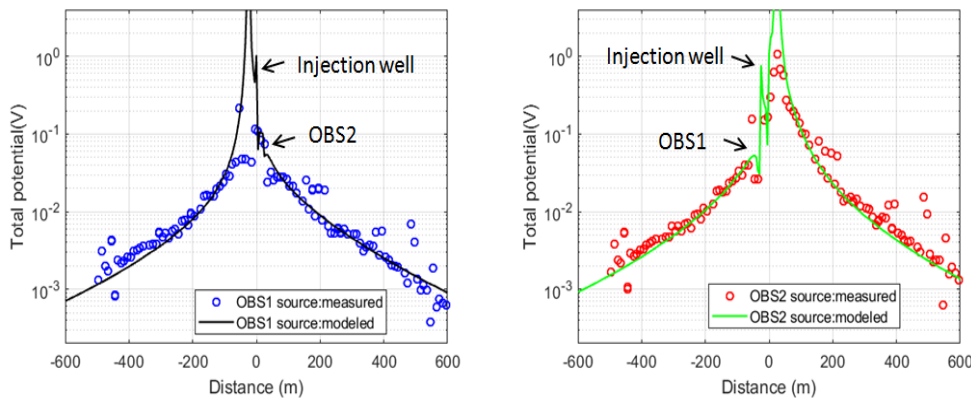


Figure 7: Fit of Numerical models to field results at CaMI. Left panel shows data fit to OB1 profile, right panel shows fit to OB2 profile.

Comparison between the electrostatic response and the broadband field data is also favorable (Figure 8). We note that the field data are electric fields measured by 10 m electrode spacing, whereas the model results assume 1 m spacing – hence the measured data are (expectedly) smoother than the modeled data. We demonstrate here, that the DC results may be a reasonable approximation to the broadband EM data collected at CAMI. If this approximation continues to hold, then the extreme computational efficiency offered by the hierarchical modeling used in the DC simulations will permit us to explore far more model complexity, especially the pervasive and troublesome data artifacts that arise when doing EM surveys in mature, culturally developed sites.

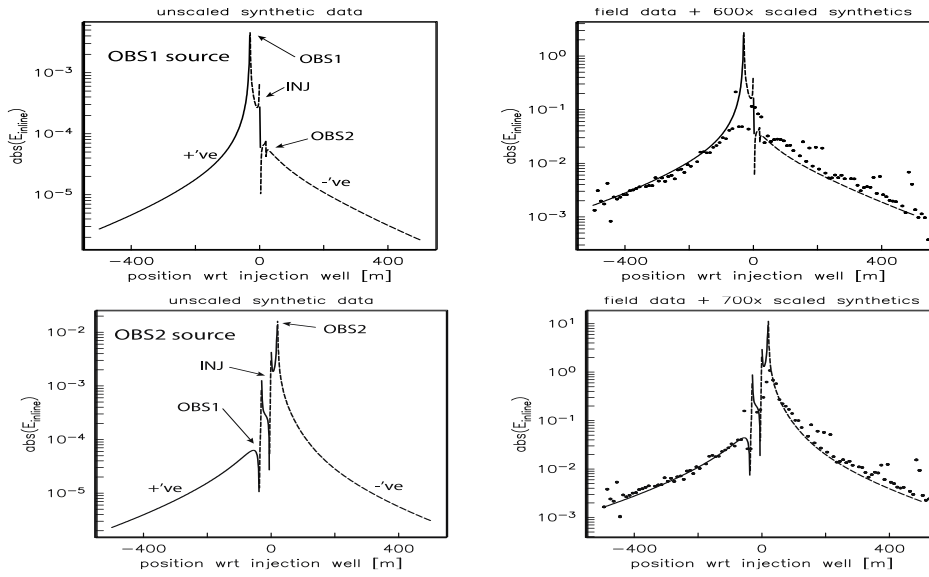


Figure 8: Magnitude of electrostatic field along the measurement profile for excitation of OBS1 (top) and OBS2 (bottom) wells. Model results (left) for each well excitation show a significant casing effect, thus justifying its inclusion in the calculation.

3.2 Seismic Oil Field Modeling:

In addition to the low frequency EM modeling, seismic modeling simulations were also conducted. We constructed a model of a well using the properties from an existing well in a California oilfield (Figure 9). A finite difference code was used to simulate the propagation of seismic waves due to a disturbance at the well head. As in the majority of wells, there were several changes in the outer diameter of the well as a function of the well depth. Because the changes in diameter were of the order of 5 cm, that was the minimum grid spacing used in the model. The well was almost 400 meters in depth and the lateral boundary must extend that far in order to avoid artificial reflections. Therefore the grid is 6000 by 10000, resulting in a model with 60 million grid blocks. A total of 1 million time steps were required for each second of simulated time. The wave fields corresponding to simulation times of 0.07s and 0.7s are shown below in Figure 10. Note the complicated multiple reflections caused by the nested well casing. The dominant feature is a tube wave propagating down the well bore. This is the wave that we are using in the project to assess the health of the well.

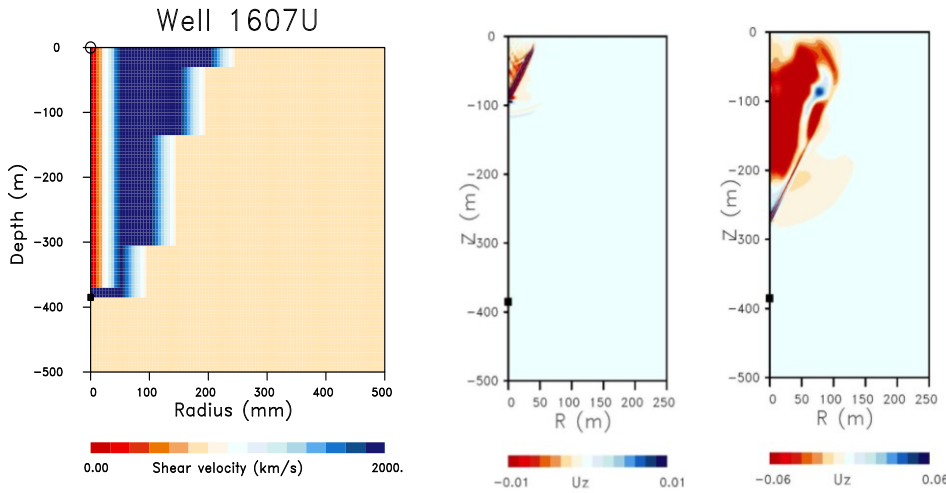


Figure 9: Shear velocity for a realistic well model (left panel) and wavefields 0.07 s and 0.7s after the initiation of an impulsive source at the ground surface (right panels).

In addition to simulating the tube wave, numerical tests were conducted to understand changes in seismic field surrounding the borehole due to breakage of the casing and water leakage. We have implemented 3D elastic code in Laplace-Fourier domain to estimate the elastic fields generated by tube waves on broken casing (Figure 10). The modeling simulates a casing break that causes water leakage through the cement and thereby creates low velocity regions. These regions can be a source of tube waves, and wavefield scattering and are registered on the surface. We performed simulations of the elastic field at frequency 50 Hz for the well broken at the depth 35 m (well shift for 16 cm and water leakage around 2 meters). The simulation results presented on Figure 10 show detectable differences in the simulated seismic wave fields when the casing is compromised. Combined with the tube wave simulations, these results suggest possible dual modality casing integrity monitoring with the seismic method.

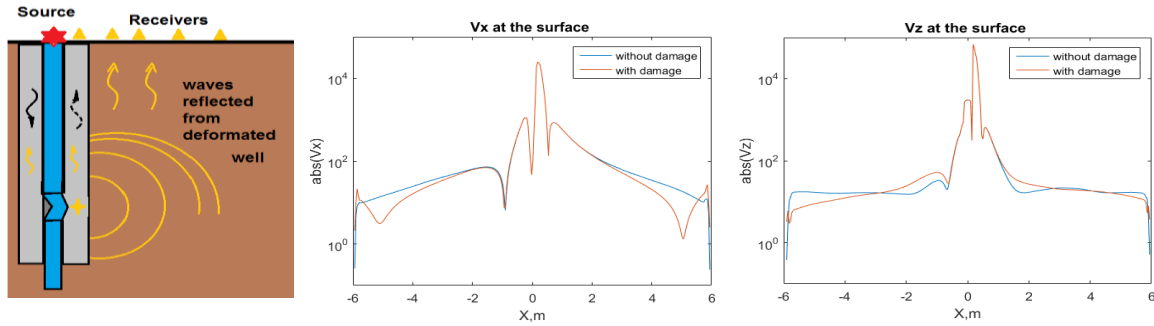


Figure 10: Left: geometric setup of the borehole breakage; Middle/right: Associated seismic simulation showing x (middle) and z (right) velocity amplitudes on the earth surface plotted are over the well.

CONCLUSIONS

A new generation of advanced borehole monitoring tools is needed to improve the current state of wellbore integrity assessment. Such tools need to provide fast, non-intrusive and cost-effective assessment of borehole state of health in order to support planning and decision-making. Our efforts to develop such tools started with numerical simulations of the geophysical signals associated with steel wellbores to understand its sensitivity to borehole condition. Our first field campaign was conducted to collect data to test the sensitivity of EM measurements to borehole completion and to validate our codes. This was successful completed and we in turn learned the influence of adjoining infrastructure on our data. Numerical modeling of the seismic tube wave propagation and associated seismic field alteration due to borehole damage and fluid leakage also showed their sensitivity to borehole degradation and potential to be used jointly with the low frequency EM methods for borehole state of health monitoring. Further tests in numerical, lab and field settings are underway to validate/improve these approaches, jointly with other proposed methods, including the transient EM reflectometry and the electrochemical methods.

REFERENCES

- Alexandrov, D.V., A. Bakulin, S. Ziatdinov, 2007, Reflection and transmission of tube waves in cased boreholes with layers and perforations, SEG Technical program expanded abstract, 10.1190/1.2793118
- Amir, N., O. Barzelay, A. Yefet, T. Pechter, 2010, Condenser tube examination using acoustic pulse reflectometry, Journal of Engineering for Gas Turbines and Power, Vol.132, 014501-1
- Conley, S., Franco, G., Faloona, I., Peischi, J. and Ryerson, T.B., 2016, Methane Emissions for the 2015 Aliso canyon Blowout in Los Angeles, Ca., Science v 351 no 6279.
- Furse, C., P. Smith, M. Diamond, 2009, Feasibility of reflectometry for nondestructive evaluation of prestressed concrete anchors, IEEE Sensors Journal, Vol. 9, No. 11, p1322-1329
- Ingraffea, A., Wells, M., Santoro, R. and Shonkoff, B., 2014, Assessment and risk analysis of casing and cement impairment in oil and gas wells in Pennsylvania, 2000-2012, Proceedings of the National Academy of Sciences of the United States of America, Vol. 111, No. 30, p10955-10960.
- Ponomarenko, A., 2008, the tube wave reflection from borehole fracture, JASS8, Sate University St. Petersburg.
- Um E., S. Kim and H. Fu, 2017, A tetrahedral mesh generation approach for 3D marine controlled-source electromagnetic modeling, Computers and Geosciences v100, 1-9.
- Weiss C J, 2017, Finite element analysis for model parameters distributed on a hierarchy of geometric simplices, Geophysics, 82, E155.
- Weiss C J and G Wilson, 2017, A new hierarchical finite element method for compact representation of oilfield infrastructure, SEG Expanded Abstracts.